International Journal of High-Rise Buildings
March 2016, Vol 5, No 1, 31-41

International Journal of
High-Rise Buildings
www.ctbuh-korea.org/ijhrb/index.php

The Use of Bracing Systems with MR Dampers in Super Tall Buildings

Aly Mousaad Aly†

Department of Civil and Environmental Engineering, Louisiana State University, 3513D Patrick Taylor Hall, Baton Rouge, LA 70803, USA

Abstract

High-rise buildings are increasingly viewed as having both technical and economic advantages, especially in areas of high population density. Increasingly taller buildings are being built worldwide. Increased heights entail increasing flexibility, which can result in serviceability problems associated with significant displacements and accelerations at higher floors. The purpose of this paper is to present the concept of a versatile vibration control technology (MR dampers with bracings) that can be used in super tall buildings. The proposed technology is shown to be effective, from a serviceability point of view, as well as resulting in dramatically reduced design wind loads, thus creating more resilient and sustainable buildings.

Keywords: Bracing systems, Dissipative analysis, High-rise buildings, MR damper, Semi-active control, Wind-induced vibration

1. Introduction

It is true that we cannot see the wind, but we can see its effects. For instance, seeing the leaves on a tree wobbling will give an indication that the weather is windy. Apart from its benefits in the field of wind energy and air pollution dispersion (moderate wind), in structural engineering, strong and extreme wind events can have devastating effects on the infrastructure. Extreme winds may cause damage to low-rise buildings in a form of window damage, roof loss, or even complete collapse of wooden structures. In tall buildings, wind can act as a friend, for instance, wind energy harvesting is favorable on high-rise buildings as per smooth and attractive wind flow that can be available in daily basis (Khayrullina et al., 2013). However, both cladding loads and the dynamics of the structure become a concern (Irwin et al., 2008). Even if the design can satisfy strength requirements, high-rise buildings are usually flexible, as per the use of high-strength lightweight materials, longer floor spans, and slender framing systems. Such flexibility leads to unfavorable vibrations that should be suppressed to avoid serious structural damage, potential failure or affected serviceability.

Vibration control of structures is an area of current research that looks promising to improve resilience, serviceability, and sustainability of the infrastructure under dynamic loads. Structural control can be achieved by various means, such as, modifying rigidities, masses, or damping, and by providing passive or active counter forces. These counter forces can be provided by passive, active, or semi-active control systems (Housner *et al.* 1997). The advantages and limitations of each scheme have been documented and the choice of which approach to use depends largely on the type of the structure, its location, the nature of the dynamic load, project commissioning, and engineering preference. Due to their low-power requirements and fail safe property, MR dampers have been enjoying renewed interest as an attractive means for protecting civil infrastructure systems against severe earthquake and wind loading (Leitmann, 1994; Dyke *et al.*, 1996; Spencer *et al.*, 1998; Goncalves *et al.*, 2006; Metwally *et al.*, 2006; Aly *et al*., 2011, Aly, 2015). Several approaches have been proposed in the literature to control MR dampers (Jansen and Dyke, 2000). Similar to viscous dampers, the challenge in using such devices in tall buildings is related to where, in a building, these devices can be installed to work effectively. In tall buildings, it is required that the damper is connected between two points where a significant displacement is expected. Unlike short and shear buildings, in which floor rotational angles are very small and there may be a significant inter-story drift under dynamic loads, slender and tall buildings may vibrate like a cantilever. It is worthy to mention that bracing systems have been used for the control of tall buildings under wind loads by several researchers (Tremblay *et al*., 2014). For instance, Kim *et al*. (2014) presents a wind-induced vibration control of tall buildings using hybrid buckling-restrained braces. The system showed significant effectiveness in vibration suppression. However, cantilever-like behavior of buildings makes it very difficult to have

†Corresponding author: Aly Mousaad Aly
Tel: +1-225-578-6654; Fax: +1-225-578-4945
E-mail: aly@LSU.edu

an effective internal bracing system (inter-story shear drift is usually not sufficient for a damper to work effectively).

The current study addresses the application of MR dampers with bracings for response reduction in super high-rise buildings under wind loads. The proposed control system combines the advantages of both active and passive control schemes and alleviates the challenge of the use of viscous and smart dampers in slender buildings. The paper presents an application case study building that has an aspect ratio of 10. Stiffness increase was first studied to investigate its effect on the response, as a direct passive control option. In addition, MR dampers with a drift magnification mechanism (DMM) are proposed. To further investigate the performance of the proposed control system, a dissipative analysis is presented.

2. Application Example

To show the applicability of using the proposed control scheme in high-rise buildings, a case study building subjected to cross-wind loads is investigated. In this section, the mathematical modelling of the building is presented, along with the wind excitation loads.

A numerical model representative of a full-scale concrete high-rise building is used in the current study. The building has a height of 221.3 m above ground and a rectangular cross-section of B/D = 2.56 (B: chord length, D: thickness). The aspect ratio is nearly 10, which makes it very slender and sensitive to strong winds. The overall building's mass is about 1.4×10^5 tons. The structure has 50 stories above ground level. There are four underground stories. A finite element (FE) model of the full-scale building was built using Midas Gen ver. 7.2.1 (Midas, 2015). Thanks to the refinement of the calculation models it is possible to analyse the behaviour of all of the competitive elements of the same member, which allow for considering the effective contribution to the total rigidity of the system supplied from every elementary member. In building up the model, the following finite elements were used: (i) plate element: to model the slaps of the floors; (ii) beam element: to model beams and pillars; and (iii) truss element: for modelling steel bars. The three-dimensional FE model represents the whole building, including the underground part. The first six natural frequencies are: 0.122 Hz, 0.135 Hz, 0.461 Hz, 0.647 Hz, 1.079 Hz and 1.083 Hz, respectively (see Fig. 1). As explained later in this subsection, this building behaves in shear in the x-direction and as a cantilever in the y-direction (very slender);

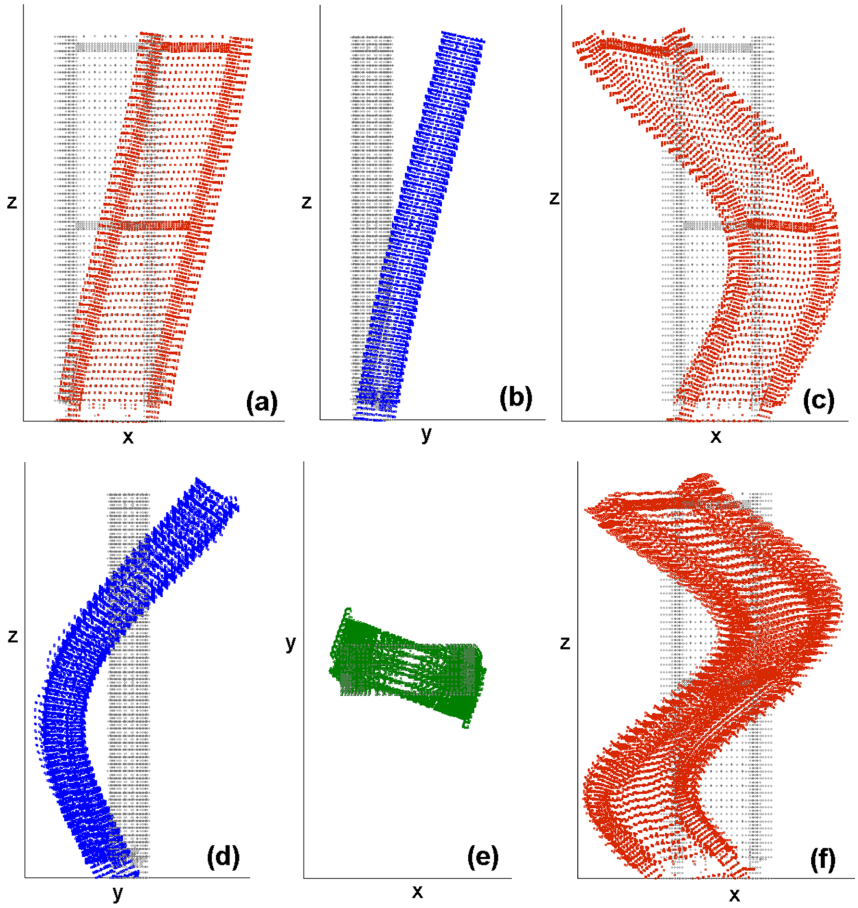


Figure 1. First six mode shapes of the building.

further description of the building is provided in Aly (2009). The current paper is focused on controlling the flexural response in the y-direction.

While mode shapes and natural frequencies can be obtained by FE modelling, it is difficult to obtain the structural damping in a similar way. This is because, unlike mass and rigidities that are distributed along structural elements, damping is related to friction between joints and some hysteresis in the material and there is no convenient way of refining the predictive capabilities regarding inherent structural damping. Accordingly, there have been some efforts to develop empirical predictive tools for damping estimation based on full-scale observations (Li *et al.*, 2002; Satake *et al.*, 2003; Smith and Willford, 2007). As a result of these efforts, Tamura and Yoshida (2008) presented a damping predictor for tall buildings that is dependent on the response amplitude. The formula for reinforced concrete buildings is given by

$$z=\frac{0.93}{H}+470\frac{x_H}{H}-0.0018 \quad (1)$$

where ζ is the first modal damping, x_H is the displacement at the top of the building, and H is the building's height. For $x_H = 0.5\ m$ and overall building height of about 240 m (including underground stories), the damping factor from the above equation is about 1%. For $x_H = 0.25$ m and 1 m the corresponding damping factors are 0.5% and 2% respectively. However, the damping factor for this building was assumed to be 1%.

Once mode shapes, natural frequencies, and damping factors are known for a high-rise building, its response can be obtained by integrating the time histories of surface wind loads with these physical parameters, for example, by using the pressure integration technique (Aly, 2013). However, for control purposes, as the control devices act together with the structure and there is a potential mode shape change due to such interaction, a lumped mass model is necessary. Consequently, a significant amount of effort was spent to create a lumped mass model, to account for the fact that mode shapes with the control devices can be different from those without control. In these lumped mass models, the behavior of the structure was a combination of shear and cantilever responses. To permit such technique of modelling, the diagonal drifts between each two adjacent floors was obtained from the lateral mode shapes. For instance, considering the diagonal length between any two arbitrary floors to be L_b, as shown in Fig. 2, this length will be $L_{b'}$ after deforming in the lateral direction, say by considering the lower mode shape in a certain direction. By doing so, the drifts can be estimated. The drift investigation study show that the building behaves mostly as a cantilever (notice significant floor rotation (Fig. 2).

The motion of the building in the transverse direction can be expressed as

$$M\ddot{x}+C\dot{x}+Kx=-F+\Lambda f \quad (2)$$

where $\mathbf{x} = [x_1\ x_2\ \ldots x_n]$ is a row vector of the displacements of the center of mass of each floor in the transverse, while

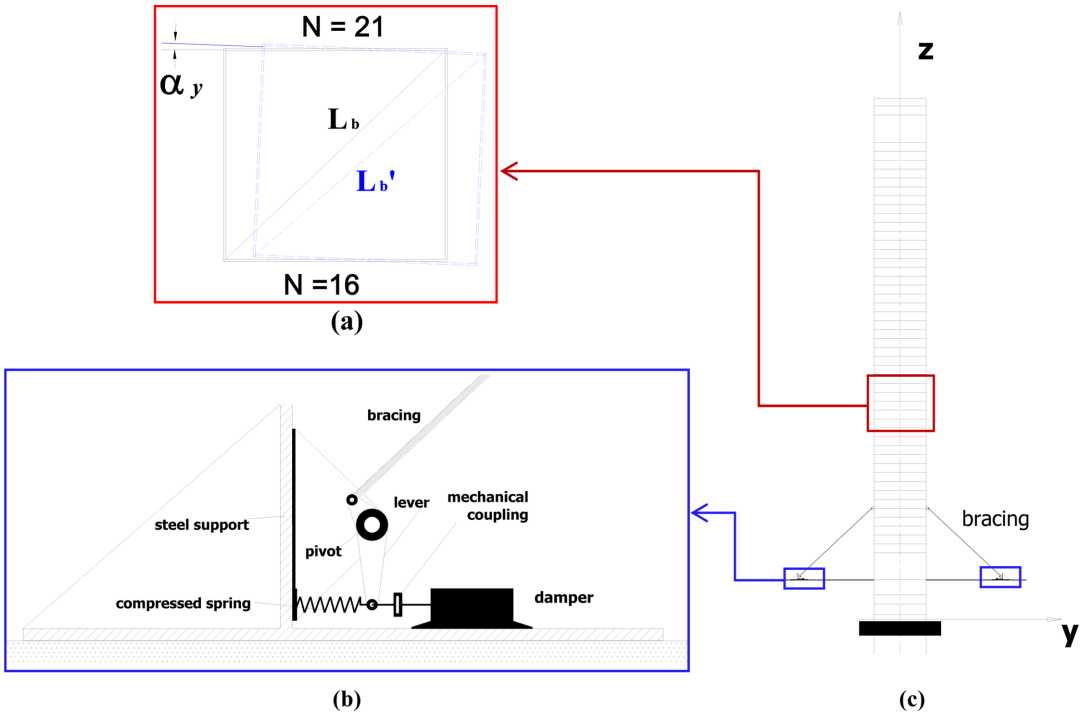


Figure 2. Configuration of dampers: (a) inter-story drift, (b) damping unit, and (c) outer bracing.

n is the number of floors. **M**, **K**, and **C** are mass, stiffness, and damping matrices, respectively. The mass matrix **M** = $diag([m_1\ m_2\ \ldots\ m_n])$ is a diagonal $n \times n$ matrix of lumped masses. The stiffness matrix **K** is obtained by assuming the stiffness between adjacent floors as a combination of cantilever and shear rigidities. MATLAB (Attaway, 2009) codes were written to derive the best stiffness matrix that provides the closest mode shapes to those of the FE model and almost the same first natural frequencies. The damping matrix **C** was obtained by considering the damping value as an equivalent Rayleigh Damping in the form of (Chowdhury and Dasgupta, 2003):

$$C = \alpha M + \beta K \tag{3}$$

in α and β are pre-defined constants. After estimating the damping matrix, the modal damping vector was obtained for all modes and the first six modal damping ratios were assigned to 1% of the critical value. Consequently, the damping matrix was reconstructed using the new modal damping vector. To obtain the damping matrix, $\mathbf{C}_s$ from the modal damping factors, the approach described in Meirovitch (1967) was followed. In Eq. (2), the disturbance **F** is a vector of horizontal wind loads acting in the lateral direction; **f** is a vector of control forces, where its coefficient matrix Λ is determined by the location of the control devices. The cross-wind loads (vector **F)** lumped at the position of the floors were obtained from a wind tunnel pressure test conducted on a scaled 1:100 rigid model of the building. The wind profile represents a typical urban terrain exposure. Further details about the wind tunnel experiment are given in Aly (2009) and Rosa *et al.* (2012).

3. Dynamic Response

Following the dynamic modelling of the building, the response can be obtained by directly integrating the equation of motion. Considering the design for serviceability, the maximum floor accelerations should not exceed a certain limit. For this building, the design criterion for serviceability is that the maximum floor acceleration for a wind with a return period of 10 years, should not exceed 20 milli-g as a peak value. However, as listed in Table 1, the response obtained is higher than the value assigned for the serviceability design. The stiffness of the building was adapted by considering a multiplication factor to the stiffness matrix in Eq. (2). The response of a structure may be controlled by modifying rigidities and/or enhancing the inherently low structural damping by implementing external mechanical systems. The first option was investigated by increasing the stiffness of the primary structure by the amounts of 10%, 20%, and 50%. As listed in Table 1, increasing the stiffness of the building by 10% may increase the acceleration response. A 20% increase in the stiffness may slightly reduce the STD accelerations, without any noticeable reduction in the peak accelerations. By aggressively increasing the stiffness of the primary structure by 50%, the accelerations are slightly reduced. To further investigate the stiffness role, Fig. 4 shows the spectra of



Figure 3. Outer bracing system.

Table 1. Acceleration response of the building in the transverse direction for different stiffness values

%age of stiffness increase	STD acceleration (milli-g)	Peak acceleration (milli-g)
0%	13.1	40
10%	14.8	53
20%	11.7	40
50%	9.8	34

across-wind loads and the corresponding across-wind building acceleration for the building with 0%, 10%, 20%, and 50% increase in the stiffness. It is shown that the acceleration response of the top floor, for instance, is contributed by lower and higher modes. The amount of increase in the reduced natural frequencies for the corresponding increase in the stiffness of 10%, 20%, and 50% are not significant to expose the building to different excitation forces.

Still the response of the building for 10%, 20%, and 50% stiffness increase significantly higher than the values prescribed by the serviceability requirements. This reveals an important conclusion, that is, stiffness increase in high-rise buildings is not a feasible solution, and may not be used for the design for comfort and serviceability. Accordingly, the second option that deals with damping enhancement through vibration control will be investigated in the following section.

4. Vibration Control by MR Dampers

4.1. MR damper configuration

While it is obvious for MR dampers to be connected between two points in a building, where significant drifts exist, in tall buildings such requirement can be barely achieved. The challenge with high-rise buildings is that the drift between adjacent floors, especially in slender buildings, is not sufficient for a damper to work properly. This can be explained by considering the modal drifts, for example, between floors 16 and 21 in the diagonal direction, where a MR damper would be connected. As shown in Fig. 2, the diagonal drifts are relatively small. For this reason, a drift magnification mechanism is considered. The proposed drift magnification mechanism consists of a lever, pre-tensioned bracing, and a helical spring to create pre-tension (see Fig. 2). Fig. 3 shows rendering and photographs of the outer bracing system. To allow for better energy dissipation, the MR damper was connected between ground and a point on the building via the drift magnification mechanism. The magnification factor (MF) is defined as

$$MF=\frac{L_2}{L_1}=\frac{x_d}{x_f}=\frac{F_f}{F_d}>1 \tag{4}$$

where L_1 and L_2 are arms of the lever; x_d is the displacement across the damper and

$$x_j=X_f cos(\theta) \tag{5}$$

in which X_f is the drift between an arbitrary floor (where the bracing is connected) and ground, θ is the inclination angle of the bracing, F_f is force acting on the floor through the diagonal bracing and F_d is the force produced by the damper. Notice that for the lever to be effective, the length L_2 (building side) should be greater than L_1 (damper side), which means MF > 1. Not only the proposed lever mecha-

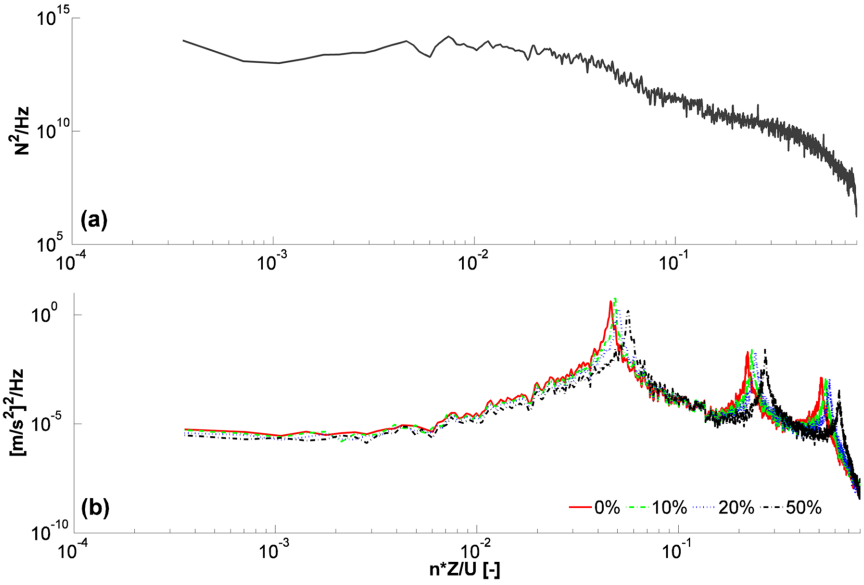


Figure 4. Wind load spectrum (a) and the corresponding acceleration response (b) for the building with 0%, 10%, 20%, and 50% stiffness increase.

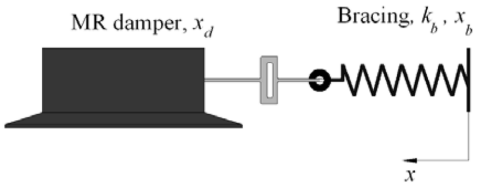


Figure 5. Modelling of the damper with bracings (Maxwell-like model).

nism can improve the performance of the MR dampers (as it increases the velocity across the damper and hence the amount of energy dissipated per cycle), but also it may reduce the required number of devices or allow to consider devices with lower damping capacity. However, this will increase control force in the bracing system, which means the need to have a stronger bracing link.

In modelling the damper bracing connection, to account for a realistic behavior of the system, the design of the bracing system is based on the assumption that the bracing members are circular steel bars with diameters that can be calculated according to the working allowable stress of the steel member. For a certain allowable stress and a known bracing length, the corresponding bracing stiffness can be found using Hooke's law

$$E=\frac{\sigma_{all}}{\varepsilon}=\frac{F_{max}L_b}{A_b\delta} \tag{6}$$

where E is the modulus of elasticity of the bracing material (about 209 GPa for steel), σ_{all} is the allowable working stress, ε is the corresponding strain, $F_{\max}$ is the maximum working force in the bracing member (including the pretension load), L_b is the bracing length, A_b is the cross-sectional area, and δ is the corresponding deflection. Eq. (6) gives the stiffness of the bracing as

$$k_b=\frac{F_{max}}{\delta}=\frac{E\,A_b}{L_b}=\left(\frac{E}{L_b}\right)\left(\frac{F_{max}}{\sigma_{all}}\right) \tag{7}$$

The deformation in the bracing element as a function of the working stress can be given by

$$\delta=\frac{\sigma_{all}L_b}{E} \tag{8}$$

For a realistic design, the bracing member is assumed to be able to carry a stress in the range of 40 MPa to 200 MPa as an overall working stress (including the pretension stress). The pretension load is assumed to be the same as the maximum capacity of the damper. Five different stiffness configurations are considered for allowable stresses of 40, 80, 120, 160, and 200 MPa.

4.2. Maxwell spring-damper model

Since the bracing is not completely rigid, the resulting assembly of the MR damper with the bracing will be similar to the Maxwell spring-damper model. The Maxwell element consists of spring and damper elements connected in series, as shown in Fig. 5. The element, massless and uni-axial, does not take into account the bending or torsion stiffness. The end points of the element can be attached to any bodies. The Maxwell element is suitable to model material responses that exhibit deformation under axial loads (Makris and Constantinou, 1991). The corresponding equations, derived for the damper deflection, x_d, bracing deflection, x_b and the total deflection, x are

$$F_d=F_b=k_bx_b \tag{9}$$

$$x=x_d+x_b \tag{10}$$

Due to the fact that the MR damper is highly nonlinear, the analytical solution of the above equations is complex. The solution to these equations is conducted numerically in SIMULINK (Attaway, 2009).

To control the response of the building, a number of MR dampers were considered. The single MR damper model has a maximum capacity of 1000 kN and mathematically modeled using the Bouc-Wen model (Yi *et al*., 1999). The equations governing the force, F_d, predicted by this model are as follows:

$$F_d=c_0\dot{x}+\alpha z \tag{11}$$

$$z=\gamma|\dot{x}|z|z|^{n-1}-\beta\dot{x}|z|^n+A\dot{x} \tag{12}$$

where z is the evolutionary variable that accounts for the history dependence of the response. The model parameters depend on the input voltage, v, to the current driver as follows:

$$\alpha=\alpha_a+\alpha_bu\;;\;\; c_0=c_{0a}+c_{0b}\;;\;\; \dot{u}=-\eta(u-v) \tag{13}$$

The parameters of the MR damper were selected so that the device has a capacity of 1000 kN, as follows (Khajekaramodin et al., 2007): α_a = 1.0872e5 N/cm, α_b = 4.9616 $\times10^5$ N/(cm.V), c_{0a} = 4.4 N.s/cm, c_{0b} = 44 N.s/(cm.V), n = 1, A = 1.2, γ = 3 cm^{-1}, β = 3 cm^{-1}, η = 50 s^{-1}. The model is simulated under a sine wave input with a frequency of 0.1 Hz (wind engineering applications) for different amplitudes (from 0.01 m to 0.1 m) for both 0 Volt and 10 Volt as indicated in Fig. 6. It is shown that the damper is able to provide the maximum damping force at a frequency of 0.1 Hz under different amplitudes of excitation. However, the amount of energy dissipated per cycle (the area enclosed in the hysteresis loop of the subfigure (b)) is increased by increasing the amplitude of the sine wave input. In practical applications, in order to increase the energy dissipated in one cycle, the velocity across the damper is to be increased. Velocity depends on the displacement amplitude and the frequency of oscillation. Since buildings oscillations under wind loads are characterized by low frequencies, one has to increase the displacement across the dam-

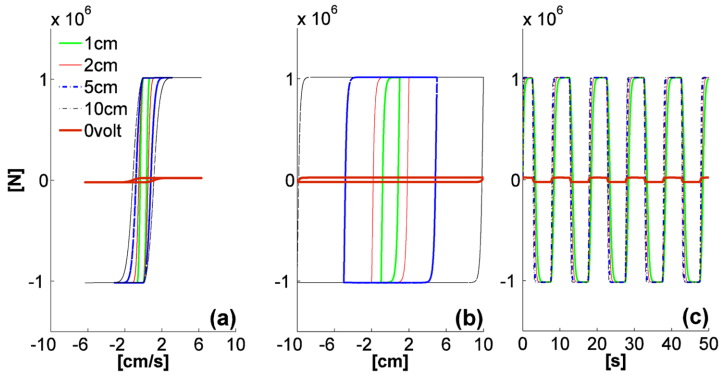


Figure 6. MR damper characteristics under sinusoidal displacement input with different amplitudes (1, 2, 5 and 10 cm) at 10 volt, and a sinusoidal displacement with a 10 cm amplitude at 0 volt.

per in order to increase the energy dissipated and hence improve efficiency.

A decentralized bang-bang controller is used with the MR dampers (Dyke and Spencer, 1997; McClamroch and Gavin, 1995). In this approach, the following control law is chosen

$$v_i = V_{max} H(-\dot{\boldsymbol{x}}^T \Lambda \boldsymbol{f}) \tag{14}$$

where v_i is the input voltage to the current driver of the i^{th} MR damper, and V_{max} is the maximum allowable voltage and $H(.)$ is the Heaviside step function. Notice that this control law requires only measurements of the floor velocities (only those in contact with the MR dampers), and the applied control forces.

4.3. Controlled response

Four MR dampers are connected with a bracing-lever system between the ground and floor 6 (Fig. 2). This configuration as well as the number of dampers, and the magnification factor was achieved by trailing several options, with the objective of minimizing the bracing length, and at the same time creating significant drifts across the dampers. A magnification factor of 3 was used. The overall deflection in the bracing system is used as an indicator of the bracings stiffness. To examine the effect of the MR dampers on the responses of the building, a bracing system with an overall deflection of 15 mm is used (about 120 MPa working stress). The stiffness of the helical spring was selected to give permit sufficient pretension in the bracing member and was assumed to be constant. This is to allow the damper to work properly all the time (i.e., to provide damping whenever the floor is moving to the right or to the left). The effect of the bracing stiffness was investigated by considering two cases (flexible and rigid), with a passive-on (constant input voltage to the current driver of the MR damper), and the decentralized control law mentioned previously. Fig. 7 shows the acceleration response for a 10 years return period and the drifts for a 100 years return period for the rigid and flexible bracing systems, for both the passive-on and the decentralized control cases, along with the original uncontrolled response. Fig. 7 indicates that both control systems are showing significant reductions in the responses of the building over the uncon-

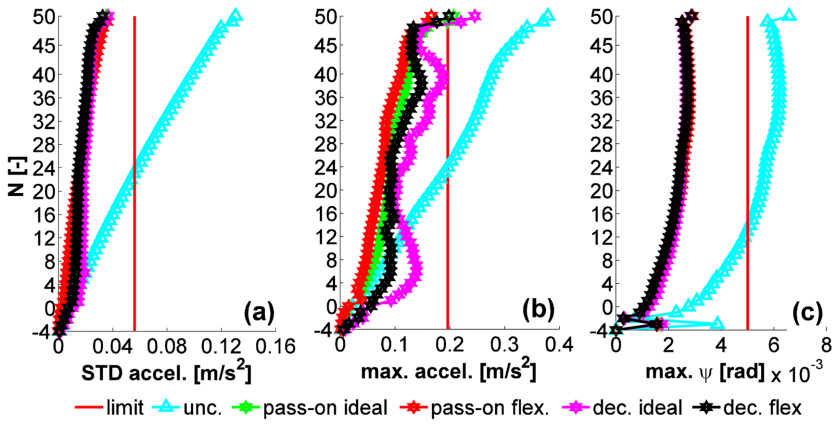


Figure 7. Acceleration response for a 10 years return period and drifts for a 100 years return period.

Table 2. Buildings responses for serviceability and safety

	Criteria	Uncon-trolled	Passive-on			Decentralized bang-bang		
		+0% Stiffness	+0% Stiffness	+10% Stiffness	-10% Stiffness	+0% Stiffness	+10% Stiffness	-10% Stiffness
I	RMS Acc. (mg)	13.0268	3.6350 (72.10%)	3.4710	3.8138	3.1292 (75.98%)	2.9582	3.3362
	Peak Acc. (mg)	37.7087	16.1623 (57.14%)	17.1560	18.4160	17.9946 (52.28%)	16.1197	20.7541
	RMS Disp. (m)	0.3496	0.1046 (70.08%)	0.0929	0.1160	0.1001 (71.37%)	0.0897	0.1116
II	Peak Disp. (m)	1.2290	0.5381 (56.22%)	0.4854	0.5637	0.5203 (57.66%)	0.4989	0.5649
	RMS Drift (rad)	0.0011	0.00057 (56.22%)	0.00051	0.00063	0.00054 (71.58%)	0.00048	0.00060
	Peak Drift (rad)	0.0066	0.0029 (56.06%)	0.0027	0.0031	0.0029 (56.06%)	0.0027	0.0030
	RMS SL (N)	1.347×10^{7}	4.711×10^{6} (65.03%)	4.5212e6	4.8032e6	4.4153e6 (67.22%)	4.2727e6	4.5132e6
	Peak SL (N)	4.864×10^{7}	2.784×10^{7} (42.76%)	2.9253e7	2.1284e7	2.5724e7 (47.11%)	2.6732e7	2.0441e7
	RMS BM (N.m)	1.994×10^{9}	6.5375e8 (67.21%)	6.2312e8	6.6876e8	6.0546e8 (69.64%)	5.8027e8	6.2344e8
	Peak BM (N.m)	6.873×10^{9}	3.759×10^{9} (45.31%)	3.6794e9	2.9540e9	3.4835e9 (49.32%)	3.6521e9	2.7948e9

I: R = 10 years, U = 28 m/s; II: R = 100 years, U = 34 m/s.

trolled case. However, the decentralized controller is showing better performance with the realistic (flexible) bracing system. The ideal (rigid) bracing decreased the performance of the decentralized controller in reducing peak accelerations, which may be attributed to the shock created by the on-off control, when the bracing is rigid. Such effect is reduced with the flexible bracing (real case), as per delay in the application of the control force to the building. This may lead to an important conclusion, that is, the on-off control performance in reducing peak accelerations for a flexible bracing system is better than that with a rigid bracing system.

Table 2 gives the uncontrolled and controlled responses of the building. Under wind loads with a return period of 10 years, MR dampers with both passive-on (constant input voltage to the current drivers of the dampers) and decentralized bang-bang controller are able to bring the RMS and peak accelerations lower than the maximum allowable values, for the assumed uncertainty in the buildings stiffness, except for the "-10% stiffness" with the decentralized controller where the peak acceleration is slightly high. However, this may be accepted as the RMS accelerations are much lower than the maximum allowable value (5.7 milli-g). The decentralized bang-bang controller is performing better than the passive-on case in reducing RMS acceleration values for the building with stiffness uncertainties which indicates the robustness of this controller (see also Fig. 8).

The results listed in Table 2 also show that, under wind loads with a return period of 100 years, MR dampers with both passive-on and decentralized bang-bang controller are capable of significantly reducing the responses of the building in the range of 42.76% to 71.56%. Increasing the stiffness of the primary structure by 10% has no significant effect on the reduction in the peak foundation bending moment; it can increase the STD values of shear and bending moment at the foundation, in addition to no significant effect on the STD values of displacement. This reveals the importance of damping enhancement in tall buildings, as means by which the responses can be signifi-

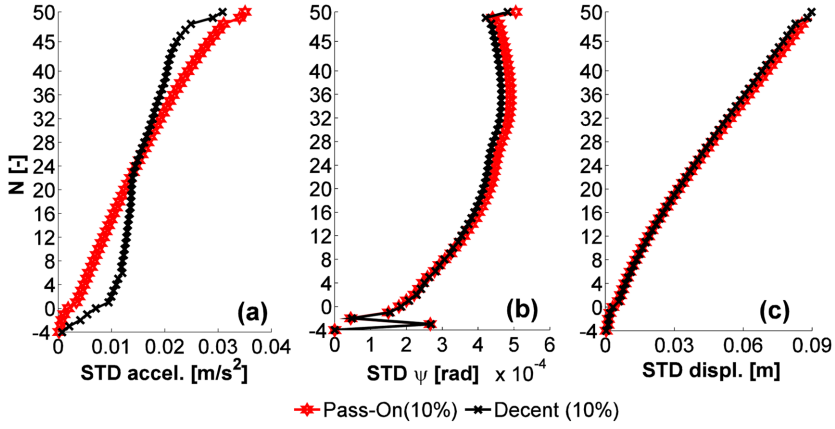


Figure 8. Accelerations for a 10-years return period and drifts for a 100-years return period obtained with the decentralized and the passive-on control cases with the MR damper.

cantly reduced, with expected lower cost, compared to stiffness enhancement. The decentralized bang-bang controller is better than the passive-on in reducing all of the RMS responses. In addition, this controller is able to reduce the peak shear loads (SL) and the peak bending moment (BM) over the passive-on case. In any case, to permit the understanding of the semi-active control strategy, a dissipative analysis is carried out in the following section.

5. Dissipativity Analysis Study

This section is about the dissipative analysis of a simplified SDOF, representative of the case study building in one lateral direction. The idea behind the study of this system is to permit the understanding of the role of the dissipative and non-dissipative forces on this simplified model in a classical way. Accordingly, the classical SDOF system was represented as shown in Fig. 9(a). The application of a generic active control force, based on the classical control theory, will result into modifications to the structural stiffness and damping by the amounts k_a and c_a, respectively, as show in Fig. 9(b). The active control force can be dissipative or non-dissipative at any certain time. To better understand this, imagine the SDOF system in Fig. 9(b) is moving from its static equilibrium position 'O' towards the extreme right hand side position 'A'. During this time (part of a full cycle), the forces developed in the spring (k_a) and the damper (c_a) are dissipative (in the opposite direction of the motion). Since the active control force is proportional to two types of gains: velocity and displacement gains (k_a and c_a), this force is dissipative when the system is moving from its 'O' to 'A'. Now imagine the system is about to move from 'A' towards 'O', the spring force is at its maximum value, while the damper force is zero. The sprig force will be in the same direction of the motion (non-dissipative) and the damper force will be in the opposite direction all time (dissipative). The damper force will increase from zero, at 'A', to a maximum value at 'O', while the spring force will decrease from its maximum value to a zero value at 'O'. This means that the total active control force (damper force + spring force) will change from non-dissipative to dissipative while the system is moving from 'A' to 'O'. If the control force is to be provided by a velocity gain only, the spring force will be zero all times and the probability that the control force is dissipative is 1. On the opposite, if the control force is provided by a displacement gain only, the control force will be dissipative over a half of the cycle (from 'O' to 'A') and will be non-dissipative over the other half of the cycle (from 'A' to 'O') giving a probability of an active control force to be dissipative to be 0.5. That is, any general control force with both velocity and displacement gains will have a probability of being dissipative with a value between 0.5 and 1. The probability that the active control force is dissipative can be expressed as a function of the properties of the primary structure (SDOF system) and the active control force (velocity and displacement gains) (Inaudi, 2000; Aly and Christenson, 2008; Erkus and Johnson, 2011). Fig. 10 shows that at relatively low control forces, the probability that these forces are dissipative is very high (close to 1). It is also shown that higher control forces have relatively lower probabilities of being dissipative. This means that an optimum active controller based on the classical optimum control theory (see Soong, 1990), will tend to modify the damping of the primary structure if the control forces are relatively low. On the other hand, an optimum active controller will tend to modify both rigidity and damping of the primary structure at relatively high control forces.

Fig. 10 shows that increasing the weight on the active control force will reduce the acceleration response significantly to some extent after that the reduction will not be significant. Now imagine the same amount of force is to be provided by a viscous damper only. The viscous damper would tend to adapt only the damping of the system all the time (the dissipative probability is 1). Fig. 10 shows that the performance of the viscous damper (Viscous) is very similar to that of the active controller (Active) at relatively low control forces. At higher control forces the performance of the viscous damper will drop significantly.

Now let's think about an ideal semi-active control force. Imagine the semi-active damper is to be turned on and off based on the value of the corresponding active control force. This approach is known as the clipped optimal control law (Dyke *et al*., 1996). Using the clipped optimal control law, the ideal semi-active control force at a certain time will be the same as the active control force, if the active control force is dissipative (smart damper turned

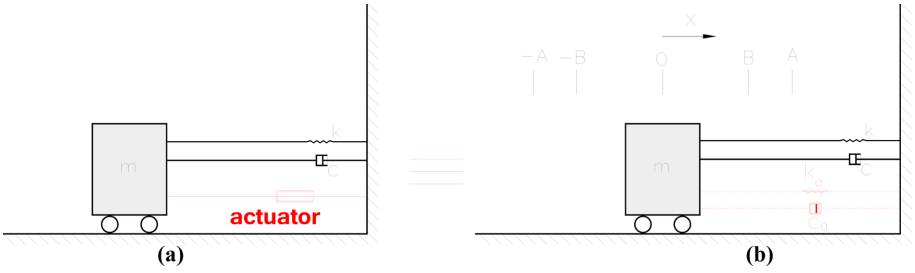


Figure 9. Effects of the control forces on the primary properties of a SDOF system.

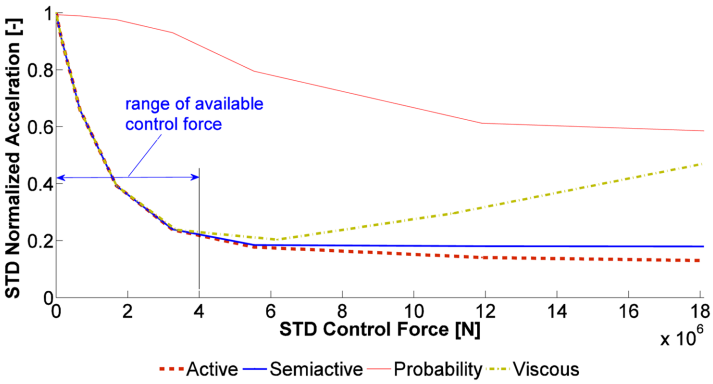


Figure 10. Dissipative analysis: the vertical axis is representative of both the normalized acceleration and the probability of control forces being dissipative (Probability).

on). When the active control force is non-dissipative, the ideal semi-active control force will be zero (smart damper turned off). This said, the semi-active control damper will only adapt the damping of the system for a fraction of time, while a viscous damper will adapt the damping all time. The active control force, however, adapts both damping and stiffness of the system all time. The performance of the semi-active system diverges from that of the active controller in the region corresponding to the decrease in the probability of dissipative forces as noted in previous studies by the author (Aly and Christenson, 2008). In addition, the figure shows that at lower semi-active control forces (corresponding to the control forces produced by the MR dampers), it is difficult to achieve much performance improvement over the passive-on case for this specific structure. However, at higher semi-active control forces the performance of the active and passive diverges and better performance over the passive-on case is expected.

The dissipative analysis shows that high-rise buildings lack significantly damping and the best control method should focus on damping enhancement, rather than stiffness enhancement. An active controller tends to modify both damping and stiffness of the primary structure in an optimal way, based on an optimization objective. For instance, when the objective is to reduce the acceleration response, the active controller tends to first increase structural damping. This can be noticed in Fig. 10 as the probability of having dissipative forces is very close to 1. Unless aggressive actuators are used, the control force is mostly dissipative by nature. Accordingly, viscous dampers (passive-on case) should provide noticeable performance, compared to active and semi-active control devices.

6. Conclusion

The purpose of this paper is to stimulate, shape, and communicate ideas with the state-of-the-art control technologies that are essential for solving wind related problems in high-rise buildings, with an objective to build the more resilient and sustainable constructions, and to optimally retrofit existing ones. The paper presents MR dampers-bracing control system for slender high-rise buildings under wind loads. The main findings are summarized as follows:

1. The results show that increasing the stiffness of the building by 10%, 20%, and 50% did not show significant response reduction benefits. That is, stiffness increase in high-rise buildings may not be a feasible solution, and may not be used for the design for comfort and serviceability.
2. Comparisons of the controlled and uncontrolled responses demonstrate the effectiveness of the proposed control system.
3. The use of lever mechanism and outer bracing offers an attractive way to control high-rise buildings.
4. The on-off control performance in reducing peak accelerations with a flexible bracing system is better than that with a rigid bracing system. The ideal (rigid) bracing decreased the performance of the decentralized controller in reducing peak accelerations, which may be attributed to the shocks created by the on-off control forces, when the bracing was assumed rigid.
5. For the purpose of using MR dampers, an on-off control of the devices may enhance their performance, compared with the passive-on case.
6. High-rise buildings have inherently low damping, which makes the priority of a control system is to increase damping rather than stiffness modification. This was better explained by the dissipative analysis carried out. The dissipative analysis shows that the decentralized control algorithm, commanding the MR dampers, is working within the possible range of optimum performance.

References

Aly, A. M. (2013). Pressure integration technique for predicting wind-induced response in high-rise buildings. *Alex.*

Eng. J. 52(4), 717-731.
Aly, A. M. (2009). On the dynamics of buildings under winds and earthquakes: response prediction and reduction. Diss. Ph. D. thesis, Department of Mechanical Engineering, Politecnico di Milano, Milan, Italy.
Aly, A. M., Zasso, A., and Resta, F. (2011). On the dynamics of a very slender building under winds: Response reduction using MR dampers with lever mechanism. *Struct. Design Tall Spec. Build*. 20(5), 539-551.
Aly, A. M. and Christenson, R. E. (2008). On the evaluation of the efficacy of a smart damper: a new equivalent energy-based probabilistic approach. *Smart Mat. Struct*. 17(4), Article ID 045008.
Aly, A. M. (2015). Control of wind-induced motion in high-rise buildings with hybrid TM/MR dampers. *Wind and Structures* 21(5), 565-595.
Attaway, S. (2009). Matlab: A Practical Introduction to Programming and Problem Solving, Butterworth-Heinemann, Amsterdam, Netherlands.
Chowdhury, I. and Dasgupta, S. (2003). Computation of rayleigh damping coefficients for large systems. *The Electronic Journal of Geotechnical Engineering*, 8, Bundle 8C.
Goncalves, F. D., Koo, J. H., and Ahmadian, M. (2006). A review of the state of the art in magnetorheological fluid technologies-part I: MR fluid and MR fluid models. *Shock Vib. Dig.* 38(3), 203-219.
Dyke, S. J., Spencer, B. F., Sain, M. K., and Carlson, J. D. (1996). Modeling and control of magnetorheological dampers for seismic response reduction. *Smart Mater. Struct.* 5(5), 565-575.
Dyke, S. J. and Spencer, J., B. F. (1997). A comparison of semi-active control strategies for the MR damper. Proceedings of the 1997 IASTED International Conference on Intelligent Information Systems (IIS '97). Grand Bahama Island, BAHAMAS, December.
Erkus, B. and Johnson, E. A. (2011). Dissipativity analysis of the base isolated benchmark structure with magnetorheological fluid dampers. *Smart Mater. Struct.* 20, Article ID 105001.
Housner, G. W., Bergman, L. A., Caughey, T. K, Chassiakos, A. G., Claus, et al. (1997). Structural control: Past, present, and future. *J. Eng. Mech. ASCE*, 123(9), 897-971.
Irwin, P., Kilpatrick, J., Robinson, J., and Frisque, A. (2008). Wind and tall buildings: negatives and positives. *Struct. Design Tall Spec. Build*. 17(5), 915-928.
Inaudi, J. A. (2000). Performance of Variable-Damping Systems: Theoretical Analysis and Simulation, 3rd International Workshop on Structural Control," Paris, France, July.
Jansen, M. and Dyke, S. J. (2000) Semiactive control strategies for MR dampers: comparative study. *J. Eng. Mech.* 126(8), 795-803.
Khayrullina, A., van Hooff, T., and Blocken, B. (2013). A study on the wind energy potential in passages between parallel buildings. 6th European and African Conference on Wind Engineering, Robinson Cambridge, United Kingdom, July.
Kim, D. H., Ju, Y. K., Kim, M. H., and Kim, S. D. (2014). Wind-induced vibration control of tall buildings using hybrid buckling-restrained braces. *Struct. Design Tall Spec. Build.* 23(7), 549-562.
Leitmann, G. (1994). Semiactive control for vibration attenuation. *J. Intell. Mater. Syst. Struct.* 5, 841-846.
Li, Q. S., Yang, K., Zhang, N., Wong, C. K., and Jeary, A. P. (2002). Field measurement of amplitude dependent damping in a 79-storey tall building and its effects on the structural dynamic responses. *Struct. Design Tall Build.* 11, 129-153.
Khajekaramodin, A., Haji-kazemi, H., Rowhanimanesh, A., and Akbarzadeh, M. R. (2007). Semi-active Control of Structures Using Neuro-Inverse Model of MR Dampers. First Joint Congress on Fuzzy and Intelligent Systems, Ferdowsi University of Mashhad, Iran, August.
Makris, N. and Constantinou, M. C. (1991). Fractional derivative model for viscous dampers. *J. Struct. Eng.* 117(9), 2708-2724.
McClamroch, N. H. and Gavin, H. P. (1995). Closed Loop Structural Control Using Electrorheological Dampers," Proc. of the American Control Conference, Seattle, Washington, p. 4173-4177.
Meirovitch, L. (1967). Analytical Methods in Vibrations. The Macmillan Co., New York.
Metwally, H. M., El-Souhily, B. M., and Aly, A. (2006). Reducing vibration effects on buildings due to earthquake using magneto-rheological dampers. *Alex. Eng. J.* 45(2), 131-140.
Midas (2015). Midas/Gen, http://www.cspfea.net/midas_gen.html
Rosa, L., Tomasini, G., Zasso, A., and Aly, A. M. (2012). Wind-induced dynamics and loads in a prismatic slender building: a modal approach based on unsteady pressure measurements. *J. Wind Eng. Ind. Aerodyn.* (107-108), 118-130.
Satake, N., Suda, K., Arakawa, T., Sasaki, A., and Tamura, Y. (2003). Damping evaluation using full-scale data of building in Japan. *J. Struct. Eng. ASCE*, 129, 470-477.
Smith R. J. and Willford, M. R. (2007). The damped outrigger concept for tall buildings. *Struct. Design Tall Spec. Build.* 16(4), 501-517.
Soong, T. T. (1990). Active Structural Control: Theory and Practice. John Wiley & Sons Inc.
Spencer, B. F., Jr., Dyke, S. J., and Deoskar, H. S. (1998). Benchmark problems in structural control. I: Active mass driver system, and II: Active tendon system. *Earthq. Eng. Struct. Dyn.* 27(11), 1127-1147.
Tamura, Y. and Yoshida, A. (2008). Amplitude dependency of damping in buildings. 18th Analysis and Computation Specialty Conference, Vancouver, Canada, April.
Tremblay, R., Chen, L., and Tirca, L. (2014). Enhancing the seismic performance of multi-storey buildings with a modular tied braced frame system with added energy dissipating devices. *International Journal of High-Rise Buildings*, 3(1), 21-33.
Yi, F., Dyke, S. J., Caicedo, J. M., and Carlson, J. D. (1999). Seismic response control using smart dampers. Proceedings of the 1999 American Control Conference (99ACC), IEEE, San Diego, CA, USA, June.